CHAPTER 74

EQUILIBRIUM PROFILES AND LONGSHORE TRANSPORT OF COARSE MATERIAL UNDER OBLIQUE WAVE ATTACK

by E. van Hijum *

Abstract. In order to obtain design criteria for artificial gravel beaches, a research programme was drawn up to study the behaviour of gravel beaches under wave attack. The present paper gives the main results of the investigations into beach formation and equilibrium profile characteristics, including the longshore transport rate of beach material under regular wave attack with varying angles of wave approach.

1 Introduction. Coarse material, such as gravel and light rubble, has recently been applied in the Netherlands as a bank protection in areas exposed to wave attack. An example is the gravel beach at the Zuidwal, the southern bank of the harbour entrance to Rotterdam (Figure 1). In order to reduce the waves inside the new harbour mouth and the connected basins, a wave-damping beach is now planned. To achieve the desired energy absorption, such a beach should consist of granular material under a small angle of inclination. For nautical and hydraulic reasons it is not possible to make the beach slope flatter than about 1:10. If loose material is used as slope protection such a slope can only be achieved by using gravel. Contrary to conventional types of bank protection, the profile of such a gravel layer will be deformed when exposed to wave attack. Data on the fluctuation of the profile under design wave conditions are required to ensure an adequate design. For this reason the Public Works Department, Harbour Entrances Division, of the Dutch Government commissioned the Delft Hydraulics Laboratory to investigate the behaviour of gravel beaches under wave attack. The tests were performed in the De Voorst Laboratory of the Delft Hydraulics Laboratory.

2 Beach formation. The process of beach formation has been described extensively by Zenkovich [1] and many others. Changes in coastline are a result of the displacement of beach material along the shore. This process is governed by the size of the material and the position of the zone in which the displacement occurs. Bottom transport, which occurs on the submarine slope under the action of waves that have not yet broken, differs fundamentally from shore transport, which takes place in the surf zone. Silt and fine sand are displaced by both wave and currents; coarser sand and gravel are affected to a lesser extent by currents, whilst larger material is displaced only by wave action. Perhaps due to percolation, gravel

* Project engineer, Maritime Structures Branch, Delft Hydraulics Laboratory, Laboratory de Voorst, The Netherlands.

beaches are rather steep: in general steeper than about 1:8. The mass of water that is formed after a wave breaks on this slope, the swash, is driven by inertia up the beach and then flows back by gravity to meet the following wave (Figure 2). The swash, which has completely lost the nature of wave motion, is exposed to the continuously interchanging forces of inertia and gravity. When the waves approach the shore obliquely, these forces operate differently. As the swash reaches its upper limit it slows down, describes a curve and flows back directly to the sea along the line of steepest gradient. Dependent on the coarseness of the material and the wave conditions, either a thin layer of material or only a few grains are set in motion. The path traversed by particles of material depends on the following factors:

- The wave conditions: wave height, wave period, angle of wave approach;
- the diameter of the particle;
- the shape of the particle and affixtures;
- the initial positions on the beach;
- the time; and
- the initial beach slope.

As an example Figure 3 shows the influence of the initial position of a particle on an equilibrium beach, beyond the breaker-line. The length of the path parallel to the coast traversed by particle 3 is much shorter than that of particle 1. The influence of the time is demonstrated in Figure 4. If the wave conditions alter, the bed will create a new equilibrium. If the waves decrease, path 1 is followed; if the waves increase, path 3 is followed and in the equilibrium phase path 2 is followed.

3 Problem schematization. In the research programme a line was followed as demonstrated in Figure 5. For correct profile development and longshore transport the sediment motion in the model had to fulfil the following conditions:

- The mechanism had to be the same as in nature, and
- in this mechanism scale effects had to be of such an order that they could be neglected.

As the mechanism of sediment transport changes completely once ripples appear, and it is up to this moment impossible to scale down this mechanism, the diameter of the material and the wave conditions were chosen in such a way that no ripples were formed.

Step 1 of the research programme, on deducing scale effects and fluctuation of the profile at perpendicular regular wave attack, has been reported in [2]. The present paper will be restricted to step 2.

4 Problem analysis. In describing profile formation and longshore transport, two groups of parameters may be composed:

a. The external parameters, characterizing the wave attack and the initial beach geometry, viz., wave height and wave length on deep water (H_o, L_o), wave period (T), depth of foreshore (h), height of beach top (k), initial slope (tg α), grain diameter (D) and angle of wave approach on the foreshore (ϕ). Because of the fact that the larger grains of a grain distribution seem to be determinant for the bed load transport, the D_{90} was chosen to characterize this grain size distribution. D_{90} means that 90% of the weight of a sample has a diameter smaller than D_{90}.

b. The internal parameters, characterizing the resulting equilibrium profile and the sediment transport during the formation of the profile. These parameters are shown in Figure 6:

h_A = height of wave run-up above the still-water level on the initial (straight) slope

h_F = height of the beach crest ≈ height of wave run-up above the still-water level on the equilibrium profile

h_B = depth below the still-water level of the point of initial movement on the initial slope

l_S and l_K = defining the position of the step or bar

l_E = defining the height of the bar

tg γ = gradient of the equilibrium profile at the still-water level

β = angle of repose under water

S(y) = mean resulting sediment transport in y-direction between two points in time. The time between these points has to be much longer than the wave period

S(x) = mean resulting sediment transport in x-direction.

For equilibrium of the external parameters in the model the Froude law of similarity was chosen. From [2] it follows that under the conditions tested the Froude law of similarity is also applicable for the internal parameters provided $D_{90} > \sim 6 \times 10^{-3}$ m. The equilibrium profile may show either a bar-type or step-type form, of which the first one has a more pronounced bar, located in the vicinity of the breaker point (see Figure 6). Appearance of a beach crest depends on the initial beach geometry and the erosion rate. If $\phi \neq 0$, than, between two points with S(x) ≈ 0, three characteristic sections can be distinguished on a beach (see Figure 7): section A (erosion), section B (equilibrium) and section C (accretion). During a test the section lengths A and C increase and section length B decreases. It is a requirement that the test is finished before section B has

vanished and after the perpendicular cross-section in B has reached an equilibrium condition. These two factors determine the minimum length of the gravel beach section.

5 Description of the model. The model, a straight beach section, was built in a wave basin with the dimensions length * width * depth = 40 * 24,5 * 1,5 m^3. The gravel section of the model beach was located between two concrete sections. A carriage with an echo-sounder could be moved over two rails parallel to the beach to make soundings of the profile. In the model two points with S(x) = 0 were made (gravel traps). Figure 8 gives a plan view of the model.

6 Tests. A summary of the test program is shown in Table 1. This table includes the two-dimensional tests from step 1. In choosing the external parameters the following four conditions were taken into account:

1. The dimensions of the wave basin.
2. The H-L diagram of Galvin [3], in order to avoid the area of secondary waves.
3. The requirement to remain below the ripple criterion.
4. The condition $D_{90} > \sim 6 * 10^{-3}$ m in order to avoid scale effects in the mechanism of the bottom transport.

Measurements were made of the waves, the wave run-up, the critical velocities at the point of initial movement of the gravel, the changes in time of the beach profile, and of the sorting of the gravel. The waves were measured in 3 rows of about 20 points each. S(y) and S(x) were calculated from frequent profile soundings, being the only way to determine these transports without disturbing the dynamical action of the gravel under wave attack. The procedure used to compute S(y) is shown in Figure 9. In section B, with $\frac{\partial S(x)}{\partial x} \to 0$, S(y) can be calculated via the continuity equation in y-direction:

$$\frac{\partial S(y)}{\partial y} + \frac{\partial z}{\partial t} = 0, \quad \text{if} \quad \frac{\partial S(x)}{\partial x} = 0.$$

In x-direction S(x) can be calculated via the continuity equation:

$$\frac{\partial S(x)}{\partial x} + \frac{\partial 0}{\partial t} = 0,$$

where 0 stands for the area of a cross-section in y-direction (see Figure 10).

7 Test results. Only the main results of the tests are given here. In Figure 11 the equilibrium conditions as reached in one of the tests is shown, together with the measured mean incident wave height in the 3 measuring rows. The symbol H_v stands for the wave height on the foreshore. The three characteristic sections A, B and C can clearly be distinguished. S(x) as function of x, in the equilibrium phase, is shown in Figure 12. S(y) as function of y, in section B, is given in Figure 13.

Summarizing all tests, the following conclusions can be drawn:

- It appears to be possible to determine an optimum initial beach profile in y-direction which shows minimum erosion and accretion for a given wave condition. Profile characteristics described in terms of the external parameters are shown in Table 2. The wave run-up on the initial slope (l_A), a vertical profile parameter (h_B), and a horizontal profile parameter (l_s) are shown in their relationships with the external parameters on the Figures 14, 15 and 16 respectively. The transition from step-profile to bar-profile is demonstrated in Figure 17. This criterion only yields for profiles in areas with $\frac{\partial S(x)}{\partial x} \to 0$. The behaviour of erosion and accretion profiles can deviate considerably, so it will be difficult to check the criterion from Figure 17 with data from beaches in nature.
- The total longshore transport of material in x-direction can be described in terms of grain diameter and design wave conditions (regular waves) by the relationships between internal and external parameters as shown in Table 2 and Figure 18. Both parameter groups in this figure are achieved by simply supposing that a layer of sediment moves along the beach with a velocity proportional to $c_b \sin \phi_b$, where c_b stands for the phase velocity of the breaking wave and ϕ_b for the angle between breaking wave and shoreline. The moving layer is supposed to have a width perpendicular to the coast proportional to l_s and a thickness proportional to D_{90}. The coefficients of proportionality appear to be related to the external parameters too. As shown in Figure 19 there exists a very poor relationship between longshore gravel transport and the so-called "energy flux". In this Figure the model conditions are enlarged with a length scale = 4. As a comparison between longshore sand transport and longshore gravel transport some measurements by Komar are also shown (from [4]).
- Sediment sorting along the equilibrium profile in y-direction seems to be a function of wave height and wave period. At low waves the coarsest material is found on the beach crest and at higher waves in the vicinity of the breaker

point. In x-direction no sorting was found.

- Measurements of critical velocities at the point of incipient motion on the initial slope support the conclusion drawn after the two-dimensional tests, indicating an increase of the critical velocity with increasing water depth.

8 Limitations in use of the results. It is clear that it is only permissible to use the obtained results within the tested range of the parameter groups. An important factor is the translation from a wind-wave field to the regular wave conditions as used in the tests. At the moment at the Delft Hydraulics Laboratory tests are being performed concerning step 4 of the research programme. In the meantime at a project in Italy (see Figure 20) good results were obtained in predicting the longshore transport rate of a natural gravel beach by characterising the wind-wave field by the significant values H_s and T_s.

REFERENCES

1. ZENKOVICH, V.P.,
Processes of coastal development.
Oliver and Boyd, Edinburgh and London, 1967

2. VAN HIJUM, E.
Equilibrium profiles of coarse material under wave attack.
14th Conference on Coastal Engineering, Copenhagen, 1974

3. GALVIN, C.J.,
Finite amplitude shallow water waves of periodically recurring form.
CERC-note, Sept. 1970

4. CERC,
Shore protection manual, 1973

grain diameter	D_{90} = 1.8; 4.4; 5.9; 7.1; 9.3; 16.5 (10^{-3} m)
(ρ_s = 2650 kg m^{-3})	D_{50} = 1.3 ; 3.4; 5.0; 6.1; 8.2; 13.0 (10^{-3} m)
wave height	0.04 - 0.47 (m)
wave period	1.20; 1.47; 1.60; 1.83; 2.00; 2.36; 2.44; (s)
angle of wave approach	0^o; 20^o; 45^o
initial slope	1:5; 1:8; 1:10
depth of foreshore	0.25; 0.40; 0.50; 0.80; 1.00 (m)
height of beachtop	∞ and still-water level

Table 1 Summary of external parameters

internal parameters	external parameters
$h_B D_{90}^{-1}$	$c_o H_o g^{-1/2} D_{90}^{-3/2} (\cos\phi)^{1/2}$ (if < 70°)
$h_B D_{90}^{-1}$	else $H_o D_{90}^{-1} (\cos\phi)^{1/2}$
$l_S D_{90}^{-1}$	$H_o D_{90}^{-1} (\cos\phi)^{1/2}$
$l_K D_{90}^{-1}$	$H_o D_{90}^{-1} (\tan\alpha)^{-1/3} (\cos\phi)^{1/2}$
$h_F D_{90}^{-1}$	$c_o H_o g^{-1/2} D_{90}^{-3/2} (\cos\phi)^{1/2}$
$l_A D_{90}^{-1}$	$c_o H_o g^{-1/2} D_{90}^{-3/2} (\cos\phi)^{1/2}$
γ	$H_o D_{90}^{-1} (\cos\phi)^{1/2}$
β	angle of repose under water ($\sim 30^o$)
$l_E D_{90}^{-1}$	$H_o D_{90}^{-1} (\tan\alpha)^{-1/3} (\cos\phi)^{1/2}$
$S(x)\, g^{-2} D_{90}^{-1} T^{-3}$	$H_o (\cos\phi)^{1/2} D_{90}^{-1}$, $\{\tanh(kh)\}^{-1} \sin\phi$

$D_{90} > 6 * 10^{-3}$ m only!

Table 2 Relationships between internal and external parameters

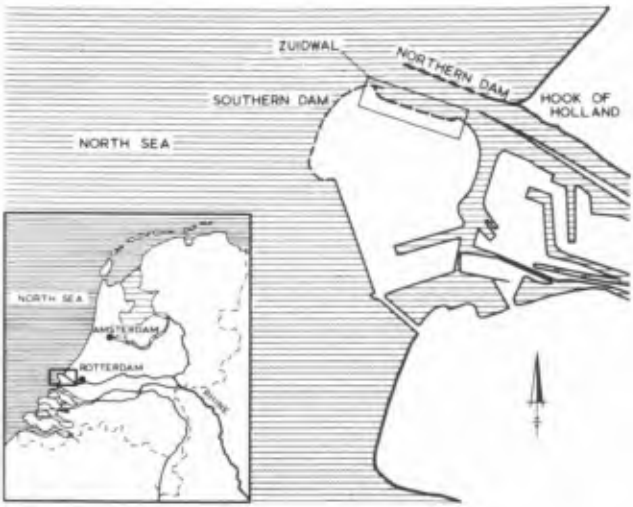

Fig. 1 Location Zuidwal

Fig. 2 Beach formation

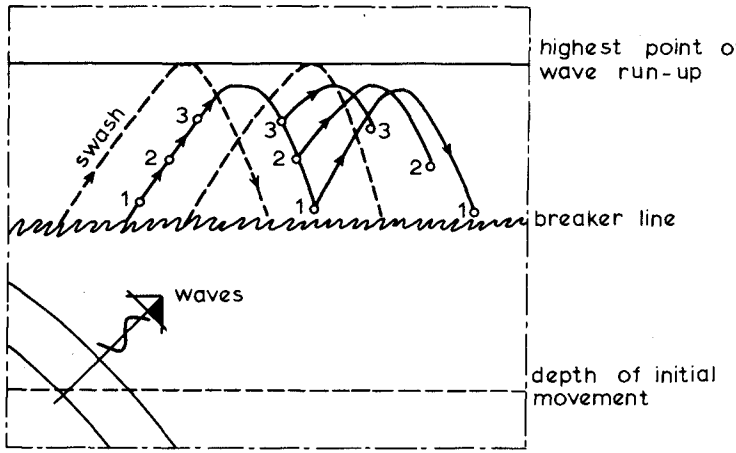

Fig. 3 Influence of the initial location on the beach on particle motion

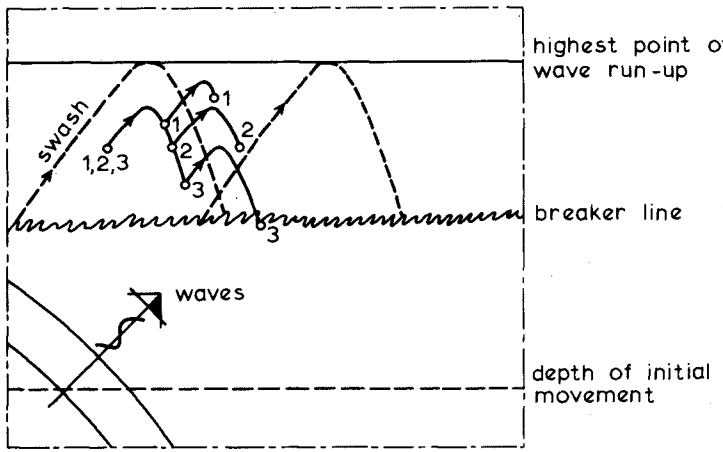

Fig. 4 Influence of the time on particle motion

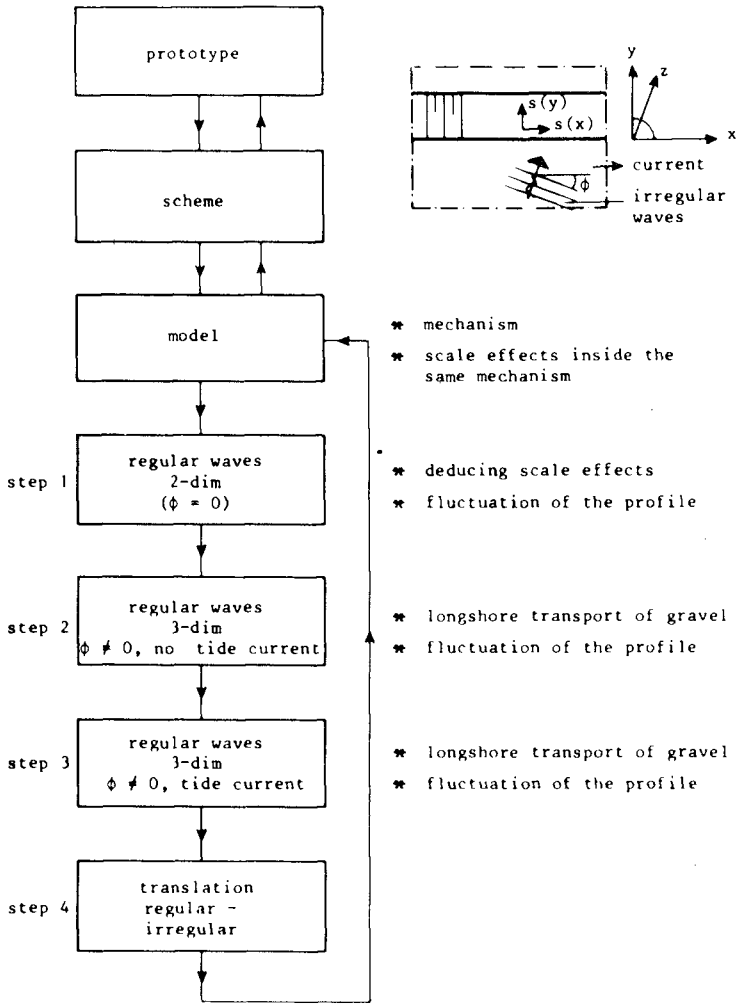

Fig. 5 Problem schematization

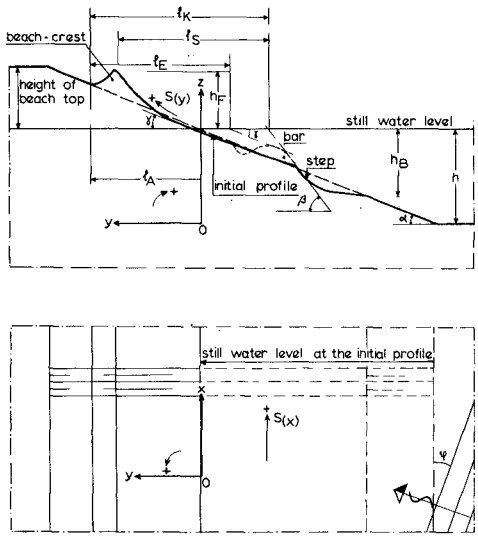

Fig. 6 Definition sketch

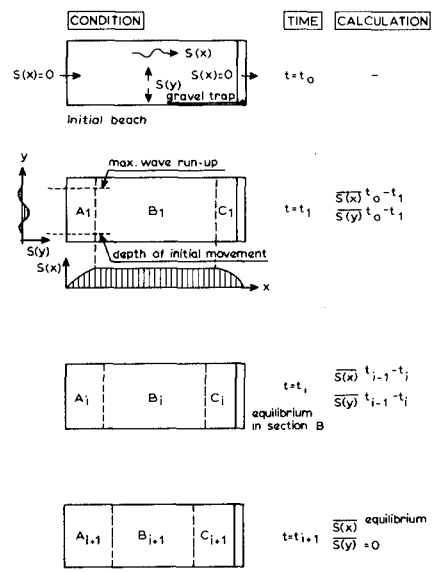

Fig. 7 Beach deformation during a test

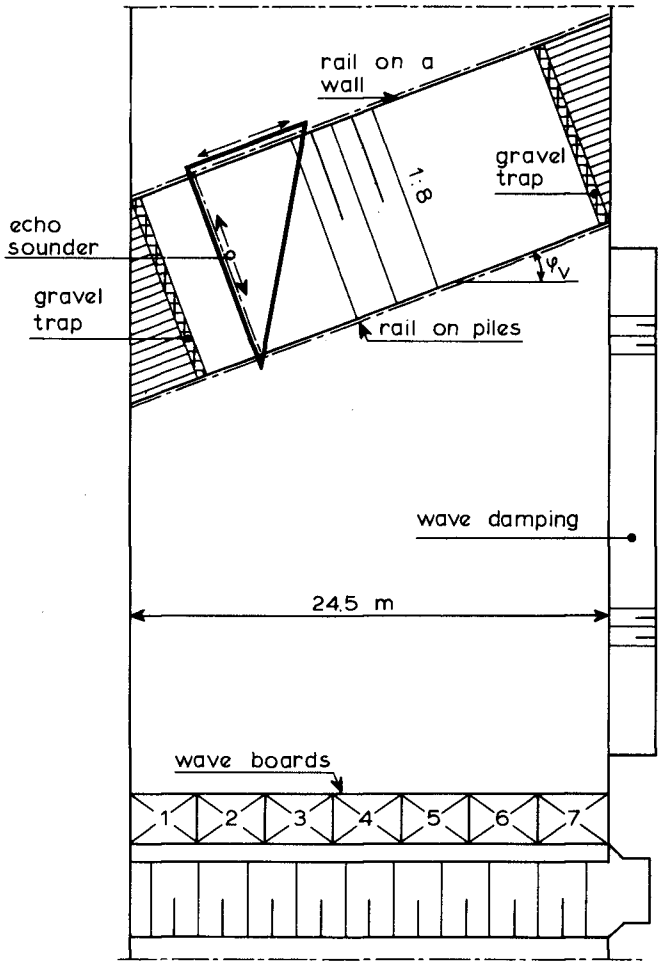

Fig. 8 Plan view of the model

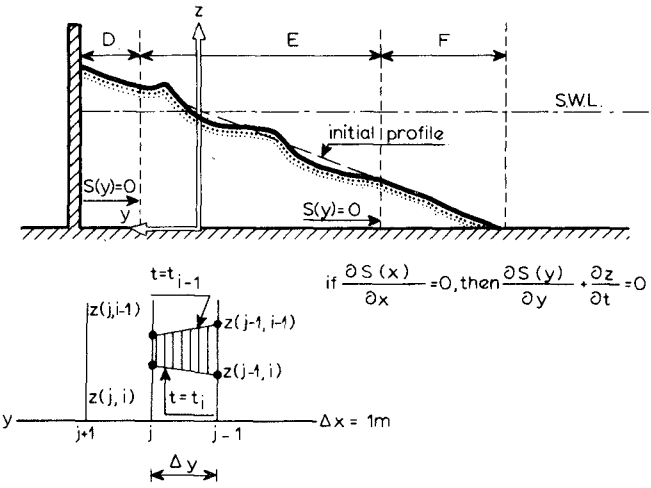

$$S(y)(j|t_{i-1}\leq t\leq t_i)=S(y)(j-1|t_{i-1}\leq t\leq t_i)+\Delta y\,\frac{z(j-1,i)+z(j,i)-z(j-1,i-1)-z(j,i-1)}{2(t_i-t_{i-1})}$$

Fig. 9 Computation of onshore-offshore transport S(y)

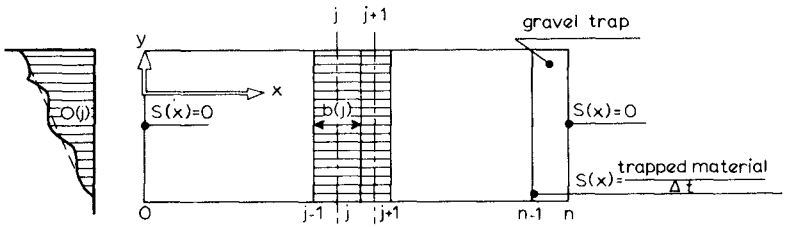

$$\frac{\partial S(x)}{\partial x}+\frac{\partial O}{\partial t}=0$$

$$S(x)(j|t_{i-1}\leq t\leq t_i)=S(x)(j-1|t_{i-1}\leq t\leq t_i)-b(j)\,\frac{O(j,i)-O(j,i-1)}{t_i-t_{i-1}}$$

Fig. 10 Computation of longshore transport S(x)

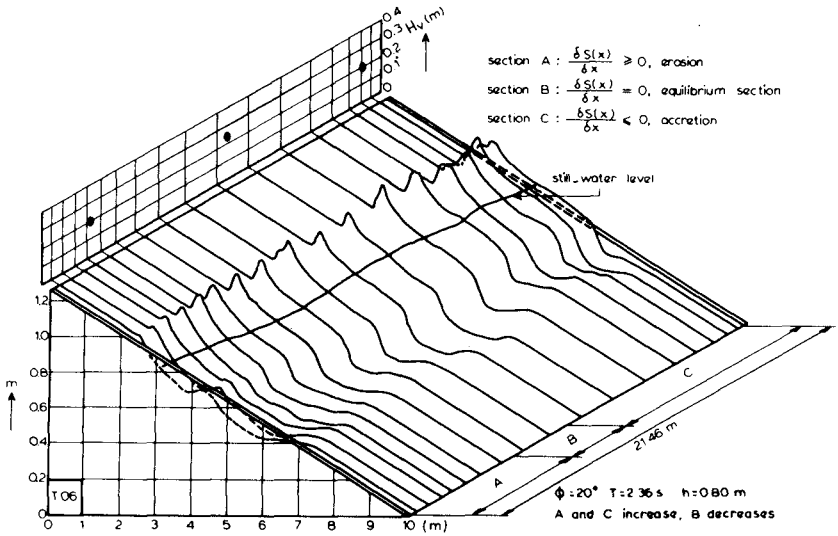

Fig. 11 Equilibrium condition

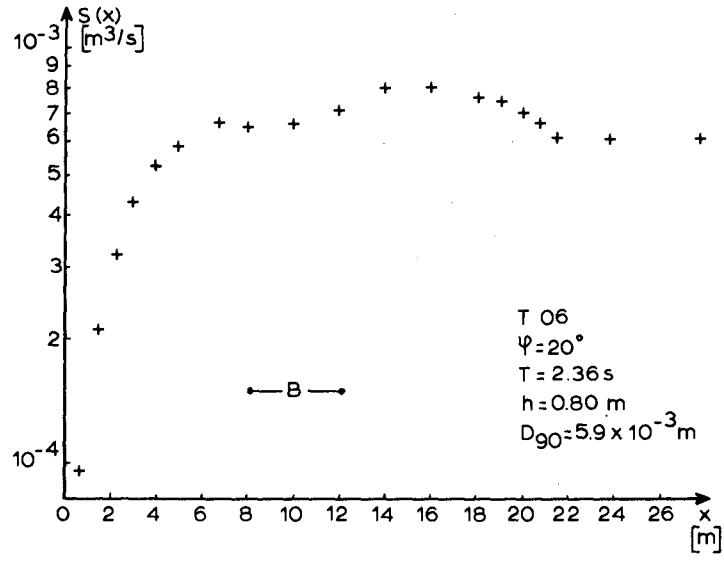

Fig. 12 Longshore sediment transport

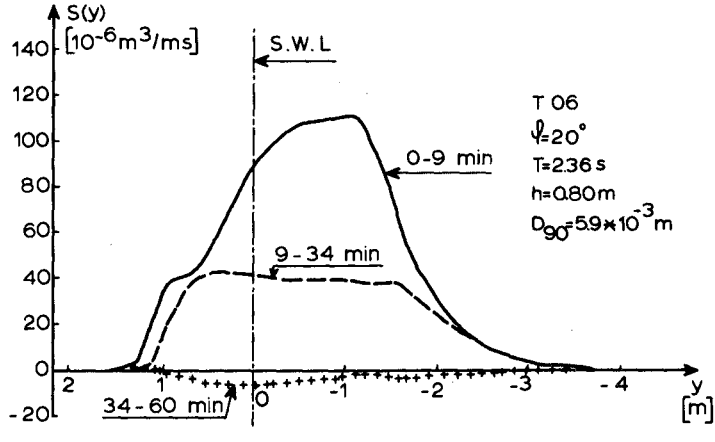

Fig. 13 Onshore-offshore transport in section B

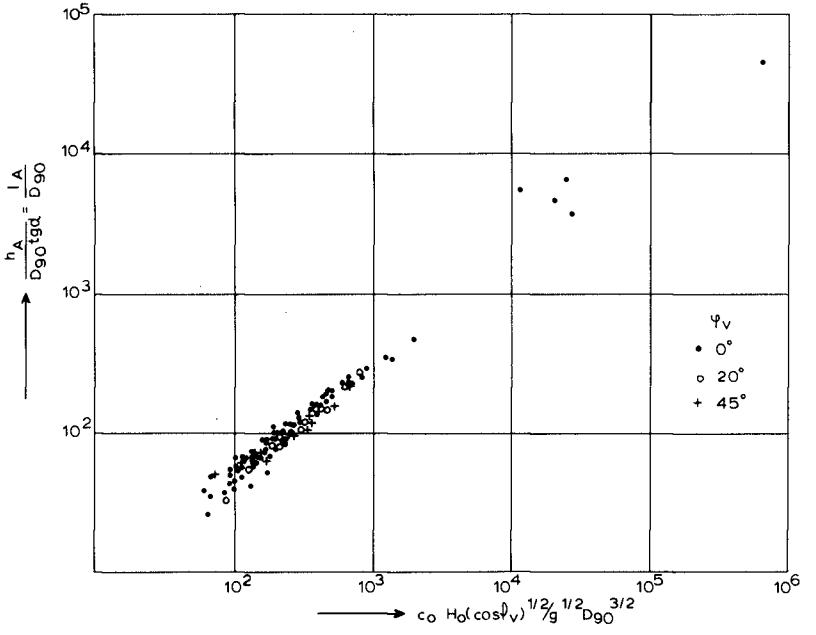

Fig. 14 Wave run-up on the initial slope

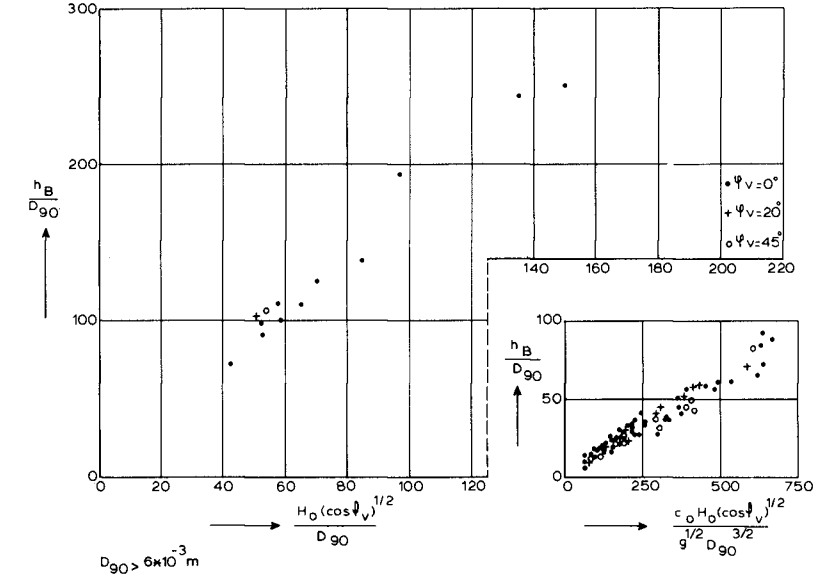

Fig. 15 Depth of incipient motion on the initial slope

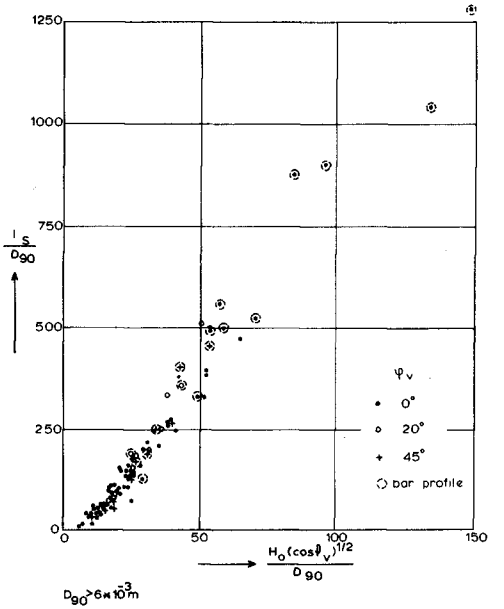

Fig. 16 Location of the step

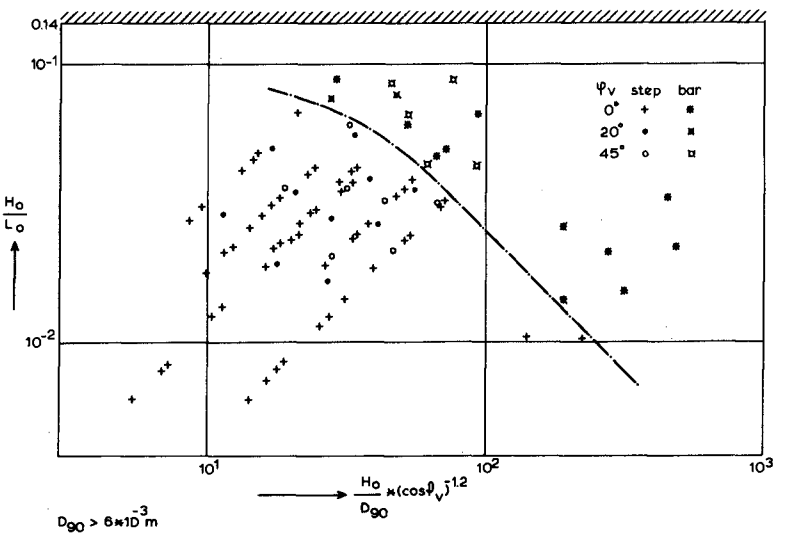

Fig. 17 Bar-step criterion

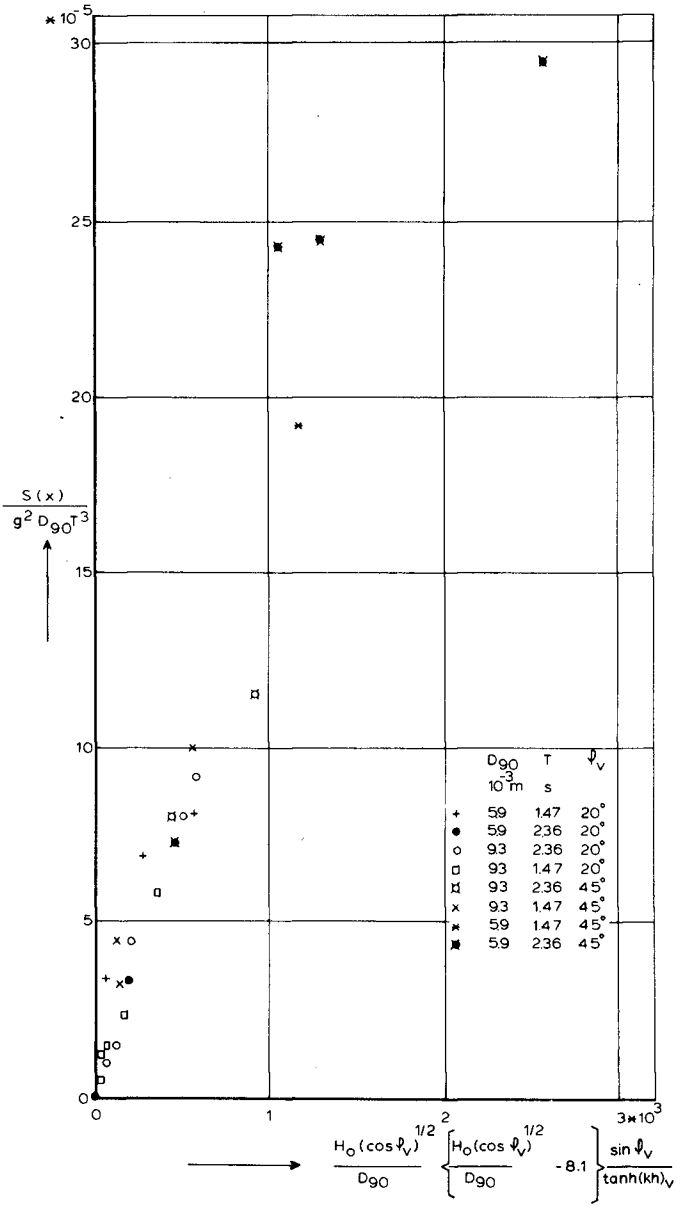

Fig. 18 Longshore transport

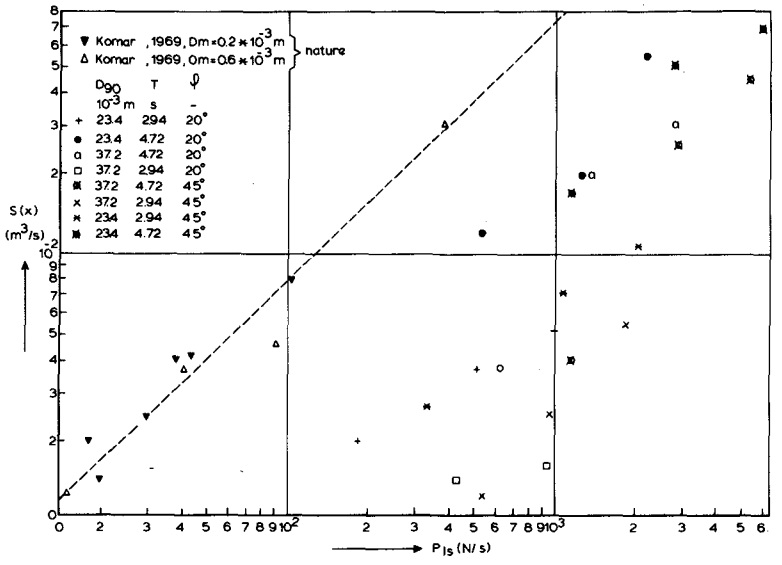

Fig. 19 Longshore transport vs. energy flux

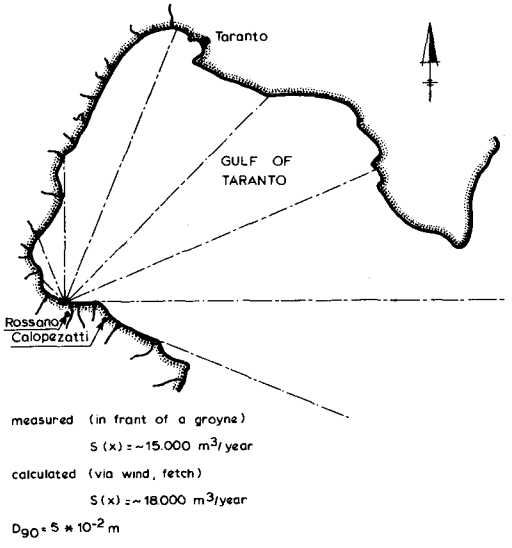

Fig. 20 Predicted and measured longshore gravel transport at Rossano beach